Laminar thermal-hydraulic efficiency of polyacrylamide solution in double pipe heat exchanger

IOP Conf. Series: Materials Science and Engineering **495** (2019) 012056 doi:10.1088/1757-899X/495/1/012056

Laminar thermal-hydraulic efficiency of polyacrylamide solution in double pipe heat exchanger

A N T Tiong[1], **P Kumar**[1] **and A Saptoro**[1]

[1]Department of Chemical Engineering, Curtin University, CDT 250, 98009, Miri, Sarawak, Malaysia

Email: angnesnt@curtin.edu.my

Abstract. This paper discusses the thermal-hydraulic efficiency of polyacrylamide (PAA) solution in a double pipe heat exchanger. This study focuses on the laminar regime, with the Reynolds number range from 250 to 2000. This research is carried out numerically through using the ANSYS Fluent software version 15.0. The overall heat transfer coefficient of PAA solution is found to be three times larger than that of water with the concentration of merely 10 ppm. This heat transfer augmentation is attributed to the purely viscous shear-thinning characteristic of the solution. However, the maximum pressure drop of the PAA solution is approximately 31.7 times greater than the value of water. The increased viscosity of the solution is the main contributor of the pressure drop increment. The pressure drop can be reduced by increasing the PAA inlet temperature. As a result of the high pressure drop of the PAA solution, its thermal-hydraulic efficiency is not as good as compared to that of water, particularly at generalized Reynolds number smaller than 1500. The flow of PAA solution is observed to have its best efficiency at the concentration of 10 ppm, generalized Reynolds number of 2000 and PAA inlet temperature of 313.15 K. The best performance index obtained is approximately 1.108.

1. Introduction

Polymer was first discovered by Toms [1] as an effective drag reducing agent in turbulent flow. Following that, extensive research was conducted on polymer. The commonly studied polymers in a pipe flow include carboxymethylcellulose (CMC), polyethylene oxide (PEO), polyacrylamide (PAA), xanthan gum (XG), hydroxyethylcellulose (Natrosol) and polyacrylic acid (Carbopol). McComb and Rabie [2] noticed that the turbulent pressure drop of water was reduced by 60-70% with the presence of 10-100 ppm PAA and PEO additives. Moreover, Escudier and Smith [3] who examined the flow of 0.125% PAA solution in a square duct found that a drag reduction up to 70% was achieved.

Besides reducing drag, the polymer solution was reported to reduce heat transfer in the turbulent regime [4-6]. The experimental results of Gupta et al. [4] showed that 0.45% PAA solution reduced the drag and heat transfer coefficient by 36% and 90%, respectively. Moreover, Debrule and Sabersky [5] claimed that 50 ppm PEO solution could decrease the heat transfer coefficient of a rough tube by a factor of 10 along with a drag reduction of a factor of 6. Kwack et al. [6] found out that the friction and heat transfer of 5 ppm PAA solution was reduced by approximately 30% and 46%, respectively. All these three groups of researchers deduced that the heat transfer reduction of polymer solution was larger compared to its drag reduction.

In addition to the studies carried out in the turbulent regime, investigations were also done for polymer solution in the laminar regime. Polymer solutions behaves differently in the laminar regime as they were discovered to enhance the heat transfer [7-9]. Xie and Hartnett [7] scrutinized the heat transfer behavior of two different polymer solutions in a 2:1 rectangular ducts. Their results indicated that both Carbopol and PAA solutions augmented the Nusselt number of water by two to three times larger. Besides, Ismail and Karim [8] stated that for a flattened tube heat exchanger with an aspect ratio (height/width) of 0.625, the heat transfer of PAA solution was improved by 86%. These researchers [7-9] agreed that the laminar heat transfer enhancement achieved by polymer solution in the non-circular ducts was attributed to the presence of secondary flow induced from the elastic property of the polymer. Numerical studies were also conducted to inspect the laminar heat transfer behavior of polymer solution in the non-circular ducts [10-12].

For circular laminar flow, the polymers were reported to behave like purely viscous fluid [9, 13-14]. They ascertained that the elastic property of polymers had negligible effect on their heat transfer performance and flow behavior. Compared to the many works done on the polymers for the turbulent and laminar non-circular flow, less attention is given to look at the heat transfer and flow characteristic of polymers in the laminar circular flow. Therefore, it is the objective of this research to address this gap by studying the heat transfer and flow behavior of polymer solution in the double pipe heat exchanger for laminar regime. The heat transfer and pressure drop results obtained will give a clearer insight on the thermal-hydraulic efficiency of polymer solution in circular flow.

2. Computational fluid dynamics (CFD) modelling

2.1. Geometries studied

A double pipe heat exchanger with the length of 1.50 m was used to study the heat transfer and flow behavior of polymer solution. Its dimensions are shown in table 1. The polymer solution flowed in the tube while water flowed in the annulus side of the heat exchanger.

Table 1. Dimensions of double pipe heat exchanger.

Double pipe heat exchanger	**Dimension**
Number of tube pass	1
Tube inner diameter, d_{i} (mm)	17.12
Tube outer diameter, d_{o} (mm)	21.34
Annulus inner diameter, D_{i} (mm)	33.40
Annulus outer diameter, D_{o} (mm)	42.72
Length, L (m)	1.50

2.2. Governing equations

In this study, the flow was assumed to be laminar, steady and incompressible. The Reynolds number range considered was from 250 to 2000. Besides, both the viscous dissipation of thermal energy and the natural convection were not taken into account in this analysis. There was negligible heat loss to the surrounding. The double pipe heat exchanger was also assumed to be smooth with zero roughness. With the assumptions made, the conservation equations of mass, momentum and energy are expressed as follows:

$$\nabla \cdot (\rho \vec{v}) = 0 \tag{1}$$

$$\nabla \cdot (\rho \vec{v} \vec{v}) = \rho g - \nabla P + \nabla \cdot (\bar{\tau}) \tag{2}$$

$$\nabla \cdot [\vec{v}(\rho E + P)] = \nabla \cdot (k_{\mathrm{eff}} \nabla T) \tag{3}$$

where ρ is the fluid density, $\vec{v}$ is the velocity vector, P is the static pressure, g is the gravitational acceleration and $\bar{\tau}$ is the viscous stress tensor. In equation (3), E is the energy, k_{eff} is the effective thermal conductivity, and T is the temperature.

2.3. Thermo-physical properties of PAA solution

The polymer solution investigated was PAA solution with its concentrations ranged from 10 to 1000 ppm. Temperature-dependent thermo-physical properties were considered in this study. As the PAA concentration studied was small, hence its effect on the density, heat capacity and thermal-conductivity of water was insignificant [15]. Therefore, these properties of PAA solution were presumed to be the same as water.

For the viscosity of PAA solution, it was predicted using the non-Newtonian Carreau model as demonstrated in equation (4). In equation (4), $\eta(\dot{\gamma})$ is the viscosity and $\dot{\gamma}$ is the shear rate. For the parameters of the Carreau model, η_∞ is the infinite-rate viscosity, η_o is the zero-rate viscosity, λ is the characteristic time, and n' is the rate index. Each of these parameters was a function of temperature, as shown in equations (5) to (8). The constants for these parameters were obtained from a rheological study which was carried out prior to this numerical study. The viscosity of PAA solution was written as user defined function for the simulations.

$$\frac{\eta(\dot{\gamma}) - \eta_\infty}{\eta_\text{o} - \eta_\infty} = \frac{1}{[1 + (\lambda\dot{\gamma})^2]^{(n')/2}} \tag{4}$$

$$\eta_\infty = \text{A}_1 + \text{A}_2\left(\frac{1}{T}\right) + \text{A}_3\left(\frac{1}{T}\right)^2 + \text{A}_4\left(\frac{1}{T}\right)^3 \tag{5}$$

$$\eta_\text{o} = \text{B}_1 \exp^{[\text{B}_2(1/T)]} \tag{6}$$

$$\lambda = \text{C}_1 + \text{C}_2\left(\frac{1}{T}\right) + \text{C}_3\left(\frac{1}{T}\right)^2 + \text{C}_4\left(\frac{1}{T}\right)^3 \tag{7}$$

$$n' = \text{D}_1 + \text{D}_2\left(\frac{1}{T}\right) + \text{D}_3\left(\frac{1}{T}\right)^2 + \text{D}_4\left(\frac{1}{T}\right)^3 \tag{8}$$

2.4. Boundary conditions

The PAA solution flowing in the tube side was cooled by the water flowing in the annulus. The counter-current flow type was examined. The velocity profile was uniform at the inlet with the flow of both PAA solution and water normal to the domain boundary. At the inlet, the velocity of PAA solution was calculated based on the value of Reynolds number while the water flow rate was set at 5 L/min. The no slip condition was applied. Besides, the working temperatures of PAA solution studied were from 313.15 K to 323.15 K. The water entered the heat exchanger at the room temperature. Moreover, the pressure outlet condition prevailed at the outlet. Insulation was imposed at the outer wall of the annulus.

2.5. Numerical solution strategy

The conservation equations and the boundary conditions were solved through finite volume method using the CFD software ANSYS Fluent version 15.0. A segregated pressure-based solver was utilized with the double precision option activated to adjust the heat transfer rate in the simulations. Furthermore, the Semi Implicit Method for Pressure Linked Equations (SIMPLE) algorithm was employed to resolve the coupling of momentum and continuity equations while the least squares cell-based gradient was adopted to handle the spatial discretization. The second order and second order upwind scheme were applied to counter for the discretization of the pressure terms as well as the

energy and momentum terms, respectively. In addition, for the convergence stability, the under relaxation factors were taken to be at their default values. The simulations were solved iteratively until the normalized residual values of all the variables reached 10^{-6}. Another convergence criterion required the net mass imbalance to be lesser than 1% of the inlet mass flux.

2.6. Data reduction

The heat transfer rate, Q and the overall heat transfer coefficient, U are expressed by the following relations:

$$Q = mC_p(T_\mathrm{o} - T_\mathrm{i}) = UA_\mathrm{t}\Delta T_\mathrm{LMTD} \tag{9}$$

$$A_\mathrm{t} = \pi d_\mathrm{o} L \tag{10}$$

$$\Delta T_\mathrm{LMTD} = \frac{\left[\left(T_\mathrm{h,i} - T_\mathrm{c,o}\right) - \left(T_\mathrm{h,o} - T_\mathrm{c,i}\right)\right]}{\ln\left[\left(T_\mathrm{h,i} - T_\mathrm{c,o}\right)/\left(T_\mathrm{h,o} - T_\mathrm{c,i}\right)\right]} \tag{11}$$

$$U = \frac{1}{\frac{1}{h_\mathrm{s}} + \frac{1}{h_\mathrm{od}} + \frac{d_\mathrm{o}}{d_\mathrm{i}h_\mathrm{id}} + \frac{d_\mathrm{o}}{d_\mathrm{i}h_\mathrm{i}} + \frac{d_\mathrm{o}\ln(d_\mathrm{o}/d_\mathrm{i})}{2k_\mathrm{w}}} \tag{12}$$

where m is the mass flow rate, C_p is the heat capacity, A_t is the total heat transfer area and ΔT_LMTD is the logarithmic mean temperature difference. The subscripts of c, h, i and o for the temperatures represent cold, hot, inlet and outlet, respectively. In equation (12), h_i is the inside fluid film coefficient, h_id is the inside dirt coefficient, h_od is the outside dirt coefficient (fouling factor), h_s is the outside fluid film coefficient and k_w is the thermal conductivity for the wall of the heat exchanger.

The Darcy friction factor, f and the pressure drop, ΔP are defined as follows:

$$f = \frac{2\Delta P d_\mathrm{i}}{\rho v^2 L} \tag{13}$$

$$\Delta P = P_\mathrm{i} - P_\mathrm{o} \tag{14}$$

where v is the velocity. The Reynolds number of water, Re is estimated using equation (15) while generalized Reynolds number, Re' as demonstrated in equation (16) is used to calculate the Reynolds number of non-Newtonian PAA solution.

$$Re = \rho v D/\mu \tag{15}$$

$$Re' = \frac{\rho v^{2-n} D^n}{8^{n-1} K \left(\frac{3n+1}{4n}\right)^n} \tag{16}$$

$$n = \frac{\mathrm{d}\log\tau}{\mathrm{d}\log\dot{\gamma}} \tag{17}$$

$$K = 10^{(\log\tau - n\log\dot{\gamma})} \tag{18}$$

where μ is the viscosity of water, D is the diameter, n is the power law exponent (or slope of the flow curve), K is the consistency index and τ is the shear stress. The thermal-hydraulic efficiency, η is evaluated with respect to the heat transfer performance and pressure drop of the solution as in equation (19) [16-17].

$$\eta = \frac{(h)_{\mathrm{PAA}}/(h)_{\mathrm{bf}}}{((\Delta P)_{\mathrm{PAA}}/(\Delta P)_{\mathrm{bf}})^{1/3}} \tag{19}$$

where h is the heat transfer coefficient and the subscript bf refers to the base fluid (water).

3. Grid independence study

Before running the simulations of PAA solution, the appropriate mesh size was assessed. A series of simulations of varying mesh size was carried out to study the effect of mesh size on the overall heat transfer coefficient. After a grid element of 609166, the overall heat transfer coefficient became independent of the grid size. Therefore, this grid size was chosen as it gave a stable grid independent result. The variation of the overall heat transfer coefficient of different grid size from this chosen grid was depicted in figure 1.

The differences in the overall heat transfer coefficient obtained from the mesh greater than the chosen grid was within $\pm$ 0.50% of that of the chosen grid. This variation was small and thus ascertained that the chosen mesh had reached its grid independent. This grid size was employed for all the simulations.

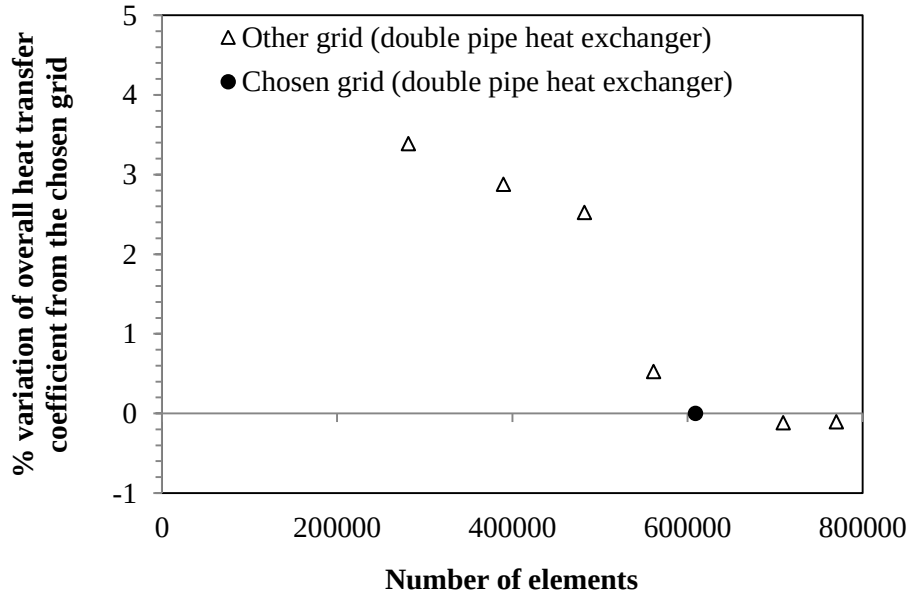

Figure 1. Grid independence study.

4. Results and discussions

4.1. Model validation

Prior to carry out the simulations of the main interest, the numerical heat transfer result obtained using water was validated with the experimental and analytical results to ensure the accuracy of the numerical solutions. The double pipe heat exchanger described in section 2.1 was the same as the experimental setup. The numerical overall heat transfer coefficient was calculated based on equation (9). The experimental value was also approximated using the same equation but using the temperatures obtained from the experiment. For the analytical value, it was estimated using equation (12). The result of comparison is presented in figure 2(a). Error bars of 10% are inserted for the experimental values. It is noticed that the numerical overall heat transfer coefficient agrees well to the experimental and analytical values, with the deviations less than $\pm$ 10%. In addition, the numerical pressure drop was also validated against the analytical value calculated from (13). Errors bars of 10%

are specified for the analytical pressure drop. From figure 2(b), it is observed that the deviations of the numerical and analytical pressure drop are within ± 10%.

The numerical results of PAA solution were also compared with the experimental results obtained using the double pipe heat exchanger. The comparison was made for the overall heat transfer coefficient of 1000 ppm PAA solution and the result is shown in figure 3. Error bars of 10% are given for the experimental results. It is seen from figure 3 that the numerical overall heat transfer coefficient is in good agreement with the experimental data. The deviation between the experimental and numerical values is approximately 0.13−4.70%.

Besides, for the friction factor of the PAA solution, the numerical results were compared with data from the correlation available in the literature. The friction factor of 1000 ppm PAA solution was compared with that of the Kozicki's power law non-Newtonian model, f =16/Re' [15]. It is noticed from figure 4 that the numerical friction factor is in very good agreement with the value from the correlation. The errors are approximately 0.07−5.47%. From all the validation done, it is concluded that the present numerical simulations give reasonably accurate results.

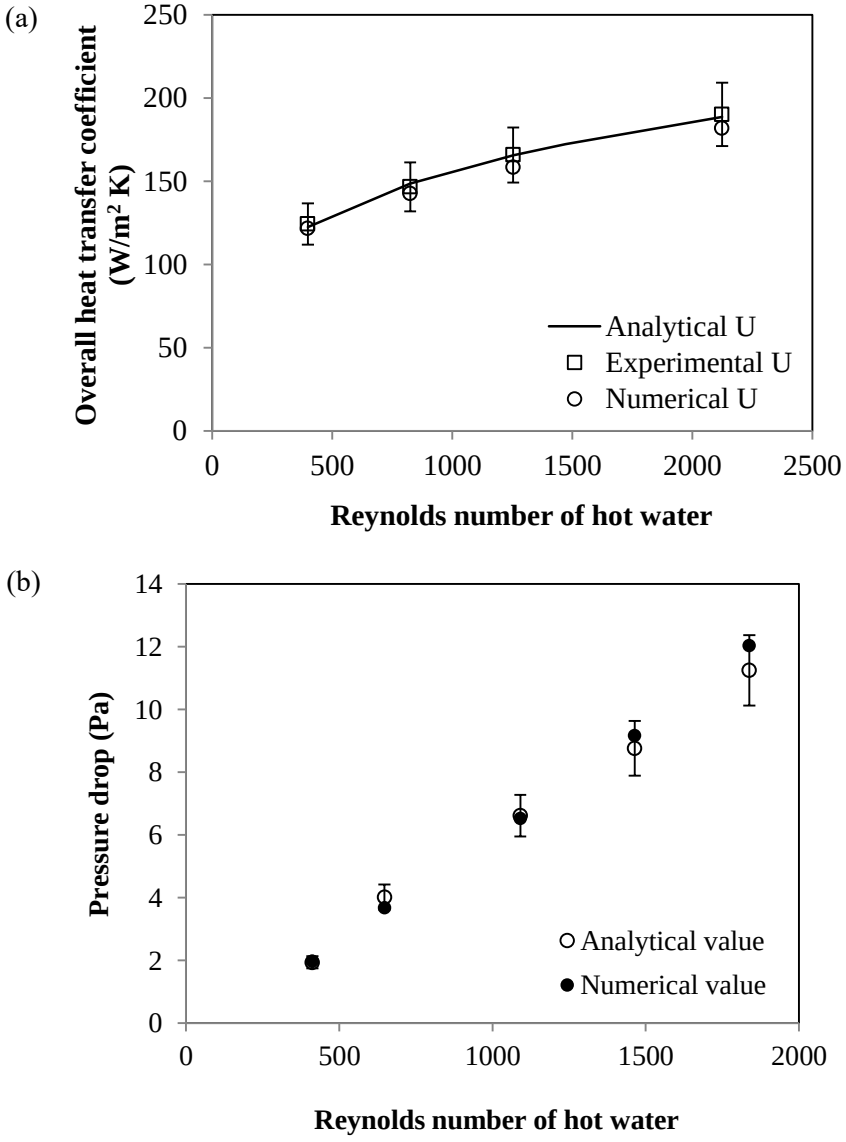

Figure 2. (a) Overall heat transfer coefficient and (b) pressure drop of water at hot inlet temperature of 313.15 K.

4.2. Heat transfer characteristic

The overall heat transfer coefficient of PAA solution is depicted in figure 5. The effect of PAA concentration on the overall heat transfer coefficient is not substantial, particularly at low concentration. The variation between the overall heat transfer coefficient of 200 and 1000 ppm PAA solution is approximately 0.21−6.52%. This difference gets smaller as the concentration reduces. This is attributed to the fact that the thermo-physical properties (except the viscosity) are the same for the PAA solution with different concentrations. The viscosity of 50 and 200 ppm PAA solution merely vary approximately 1.88 and 4.37% on average compared to that of 10 ppm PAA solution, respectively. The difference in the viscosity between 10 and 1000 ppm PAA solution is about 26.13% on average. As a result, for PAA solution with lower concentrations, the overall heat transfer coefficient achieved is similar. Besides, it is shown in figure 6 that the influence of PAA inlet temperature on the overall heat transfer coefficient is not significant. This might be because the temperature range considered in this study is not big enough to see its importance.

From figure 7, it is observed that with a low PAA concentration of 10 ppm, the overall heat transfer coefficient is improved to be three times higher relative to water. Since the only difference between the PAA solution and water is on their rheology behavior, it is postulated that this heat transfer enhancement is owing to the purely viscous shear-thinning characteristics of PAA solution. Furthermore, the viscosity of the PAA solution is higher compared to water, thus, its velocity is higher at a particular generalized Reynolds number. Higher velocity promotes larger heat transfer rate.

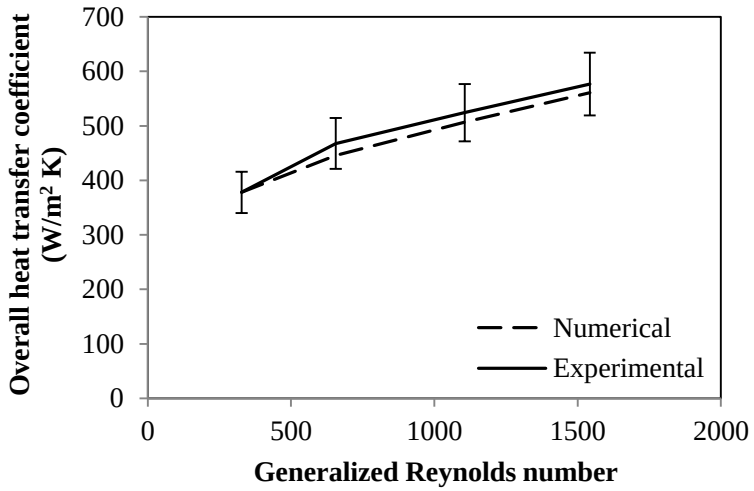

Figure 3. Comparison between experimental and numerical overall heat transfer coefficient of 1000 ppm PAA solution at hot inlet temperature of 323.15 K.

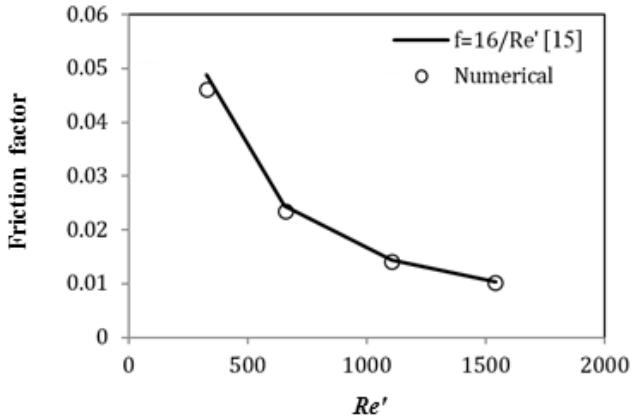

Figure 4. Comparison of friction factor for 1000 ppm PAA at hot inlet temperature of 323.15 K.

4.3. Pressure drop and friction factor

Figure 8 shows the pressure drop of PAA solution at the hot inlet temperature of 323.15 K. The pressure drop of PAA solution increases with the increasing of generalized Reynolds number. When the generalized Reynolds number increases, the increment in the flow rate leads to a higher pressure loss. From figure 8, it is also observed that the pressure drop of PAA solution increases when the concentration increases. The solution becomes more viscous when the concentration is raised. Therefore, larger shear stress is experienced near the duct wall, leading to larger pressure loss to keep the solution flowing. At the generalized Reynolds number of 2000 and hot inlet temperature of 323.15 K, the pressure drop of 1000 ppm PAA is approximately 31.7 times larger than that of water.

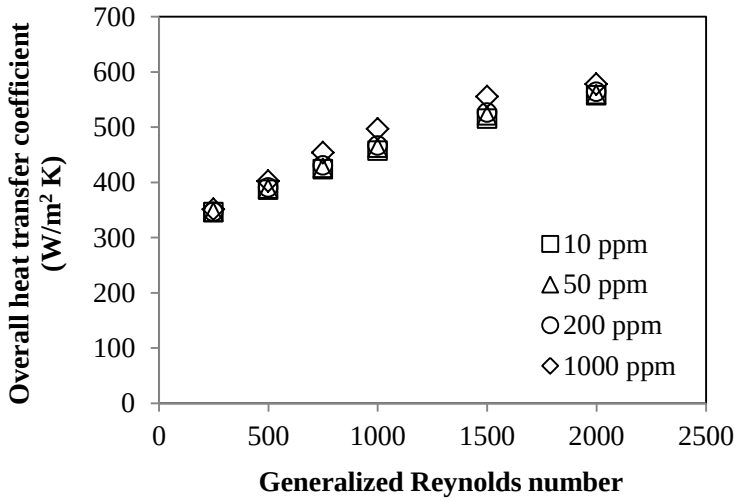

Figure 5. Overall heat transfer coefficient of PAA solution at hot inlet temperature of 323.15 K.

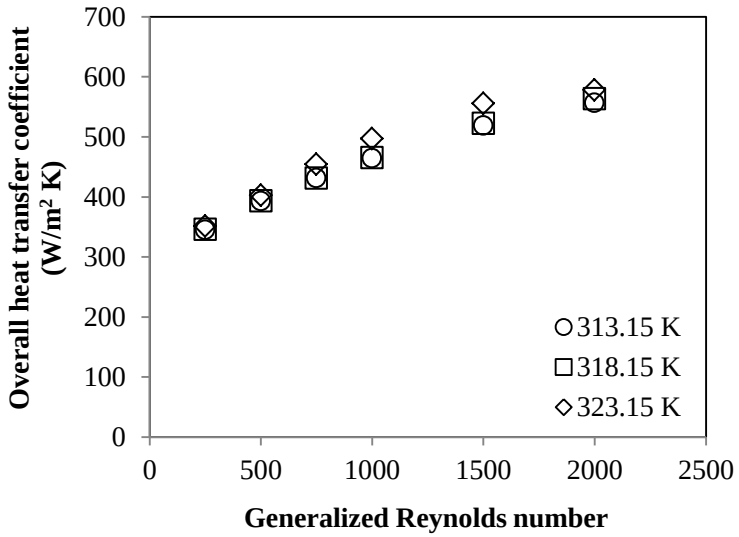

Figure 6. Overall heat transfer coefficient of 1000 ppm PAA solution.

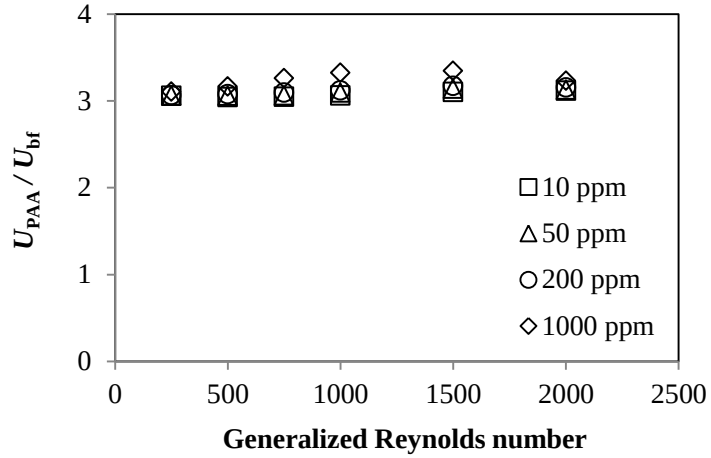

Figure 7. Ratio of overall heat transfer coefficient of PAA solution to that of water at hot inlet temperature of 323.15 K.

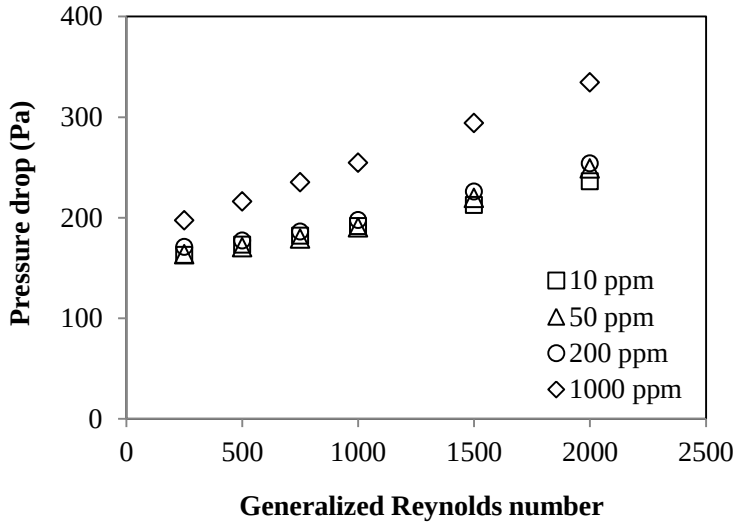

Figure 8. Pressure drop of PAA solution at hot inlet temperature of 323.15 K.

In addition, as displayed in figure 9, when the inlet temperature of the PAA solution increases, the pressure drop decreases. The reduction in viscosity occurs when the temperature of the solution increases. Higher temperature increases the motion and vibration of the liquid molecules, and this reduces the resistance of the fluid flow, so the pressure drop is lower.

The friction factor of PAA solution in the double pipe heat exchanger is depicted in figure 10. From this figure, there is a good agreement between the numerical friction factor and the value predicted from the power law, with the maximum deviation of 6.05%. This finding is similar to those obtained by other researchers [9, 13].

4.4. Thermal-hydraulic efficiency analysis

The thermal-hydraulic performance of PAA solution in the double pipe heat exchanger is shown in table 2. Generally, it can be seen from this table that the thermal-hydraulic efficiency of PAA solution increases with the increase of generalized Reynolds number but it decreases when the concentration increases. At a higher generalized Reynolds number, the $\Delta P_{PAA}/\Delta P_{bf}$ will decrease, leading to a higher thermal-hydraulic efficiency. In contrast, when the PAA concentration increases, the $\Delta P_{PAA}/\Delta P_{bf}$ will increase as well. Hence, at larger PAA concentration, the thermal-hydraulic performance

index of the solution decreases. Therefore, it is inferred that the $\Delta P_{\mathrm{PAA}}/\Delta P_{\mathrm{bf}}$ has more a dominant effect on the performance index over the relative heat transfer enhancement.

In addition, it is perceived that the temperature of the PAA solution has minor influence on the thermal-hydraulic performance. The performance index obtained for the three different temperatures studied are similar. This is because the pressure drop and the Nusselt number ratio of the PAA solution to that of the base fluid do not vary significantly with the temperature as the temperature range considered is not too big.

Overall, the thermal-hydraulic efficiency of PAA solution in the double pipe heat exchanger is not as good as that of the water, particularly at lower generalized Reynolds number. The best performance index is found to be at the generalized Reynolds number of 2000 and for 10 ppm PAA solution, which is 1.108, 1.106 and 1.105 at the temperature of 313.15 K, 318.15 K and 323.15 K, respectively.

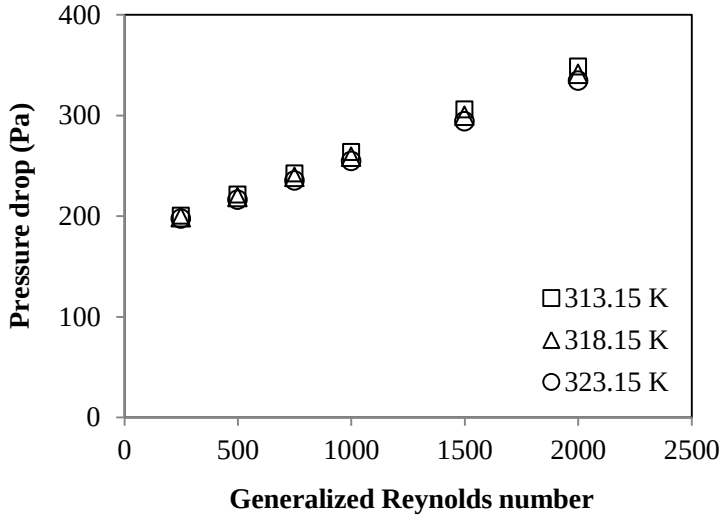

Figure 9. Pressure drop of 1000 ppm PAA solution.

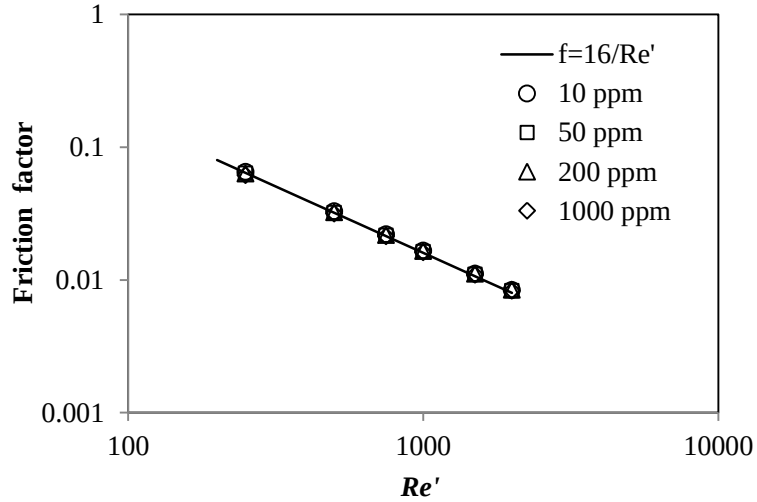

Figure 10. Friction factor of PAA solution at hot inlet temperature of 313.15 K.

5. Conclusions

This study presented the laminar heat transfer and flow behavior of PAA solution in the double pipe heat exchanger. The PAA solution flowing in the tube was cooled by the water flowing in the

annulus. From the heat transfer and flow characteristics, the thermal-hydraulic efficiency of the solution was assessed. The following conclusions had been drawn:

1. The overall heat transfer coefficient of water was improved by three times higher with merely 10 ppm PAA added to it. The main reason for this heat transfer enhancement was found to be the purely viscous shear-thinning behavior of the PAA solution.
2. Higher PAA concentration induced larger pressure drop as the viscosity of the solution increased. The pressure drop of PAA solution was maximum at the concentration of 1000 ppm and the generalized Reynolds number of 2000. This maximum pressure drop of PAA solution was 31.7 times larger than the value of water.
3. The flow of PAA solution in the double pipe heat exchanger was not as efficient as water, especially when the generalized Reynolds number was low (<1500). The thermal-hydraulic efficiency of the solution was found to be higher when the generalized Reynolds number increased and the PAA concentration decreased. The best performance index was obtained by 10 ppm PAA solution at the generalized Reynolds number of 2000, with the values of 1.108, 1.106 and 1.105 at the PAA inlet temperatures of 313.15 K, 318.15 K and 323.15 K, respectively.

It is recommended to increase the PAA inlet temperature range studied to inspect its effect on the heat transfer. Besides, the flow rate of water flowing in the annulus is constant in this study, it is also worth investigating the effect of water flow rate on the thermal-hydraulic efficiency of PAA solution. Co-current flow condition in the heat exchanger can also be considered for future study.

Table 2. Thermal-hydraulic efficiency of PAA solution.

PAA Concentration (ppm)	Generalized Reynolds Number				
	250	**500**	**1000**	**1500**	**2000**
Temperature of 313.15 K					
10	0.521	0.738	0.922	1.042	1.108
50	0.514	0.729	0.918	1.039	1.103
200	0.504	0.729	0.910	1.035	1.103
1000	0.494	0.693	0.846	0.944	0.997
Temperature of 318.15 K					
10	0.521	0.725	0.911	1.031	1.106
50	0.516	0.721	0.907	1.030	1.099
200	0.515	0.718	0.905	1.022	1.097
1000	0.495	0.683	0.837	0.937	1.005
Temperature of 323.15 K					
10	0.596	0.730	0.906	1.020	1.105
50	0.595	0.725	0.902	1.019	1.092
200	0.587	0.723	0.894	1.018	1.090
1000	0.567	0.698	0.883	0.985	1.020

Acknowledgements
The financial assistance provided by the Ministry of Higher Education (MOHE) Malaysia under the Exploratory Research Grant Scheme (ERGS) and the support from Curtin Malaysia are gratefully acknowledged.

References

[1] Toms B A 1949 *Proceedings of the 1st International Congress on Rheology* (North-Holland, Amsterdam) pp. 135-41
[2] McComb W D and Rabie L H 1982 *AIChE J.* **28** 547-57
[3] Escudier M P and Smith S 2001 *Proc. of the Royal Society of London. Series A: Mathematical, Physical and Engineering Sciences* **457** 911-36

[4] Gupta M K, Metzner A B and Hartnett J P 1967 *Int. J. Heat Mass Transfer* **10** 1211-24
[5] Debrule P M and Sabersky R H 1974 *Int. J. Heat Mass Transfer* **17** 529-40
[6] Kwack E Y, Hartnett J P and Cho Y I 1982 *Warme- und Stoffubertragung* **16** 35-44
[7] Xie C B and Hartnett J P 1992 *Ind. Eng. Chem. Res.* **31** 727-32
[8] Ismail Z and Karim R 2012 *Appl. Therm. Eng.* **39** 171-8
[9] Hartnett J P 1992 *J. Heat Transfer* **114** 296-303
[10] Naccache M F and Mendes P R S 1996 *Int. J. Heat Fluid Flow* **17** 613-20
[11] Yue P T, Dooley J and Feng J J 2008 *J. Rheol.* **52** 315-32
[12] Peres N, Afonso A M, Alves M A and Pinho F T 2009 *Congreso de Metodos Numericos en Ingenieria* (Barcelona, Spain)
[13] Cho Y I and Harnett J P 1982 *Adv. Heat Transfer* vol. 15, ed. J P Harnett and F I Thomas (USA:Elsevier) pp. 59-141
[14] Tiong A N T, Kumar P and Saptoro A 2015 *Korean J. Chem. Eng.* **32** 1455-76
[15] Hartnett J P and Kostic M 1985 *Int. J. Heat Mass Transfer* **28** 1147-55